Texture Characterization of Fine Particles Released During Thermal Shock and Combustion Processes by Fractional Brownian Motion Analysis.

Paper # 474

Eduardo F Herrera, Iván Templeton, Roberto Camarillo, Elías Ramírez, Guillermo González, Jorge I Carrillo, Ramón Gómez, Alfredo Campos, Luis Lozoya Márquez L. and Damaris Acosta Slane
Centro de Investigación en Materiales Avanzados, S.C., Chihuahua (CIMAV)
Carmen J. Navarro
Junta Municipal de Aguas y Saneamiento (JMAS)

ABSTRACT

In this paper some of the data obtained subsequently to the conclusion of the project called "New high-quality mined nanomaterials mass produced for plastic and wood-plastic nanocomposites"[1] are described. The aim of this project was to investigate the release of nanoparticles extracted during the mining process, which are functionalized to improve the properties of materials for different industrial uses. The release of these particles might cause adverse health effects mainly in developing countries, where the waste produced by these materials is not a sustainably managed, and it is indiscriminately used in burning brick ovens, among others. Our participation in the project was to identify whether there was release of nanoparticles in the thermal and mechanical processes of the production. The present study describes some preliminary results of a new approach that aims to develop a method by which the structure of the surfaces of the fine particles can be defined and classified by a specific parameter called Hurst coefficient (H) which is directly related to the fractal dimension. The proposed method uses the fractional Brownian motion (fBm) analysis to parameterize the microscopic images recorded from the released particles with various components. At the microscopic scale, the particles were segmented from the background and the values of H of the selected regions in the images were determined. The range of H values was between 0.27 and 0.60, depending the fluctuation of the surface of the particle. Finally, some future work related applications of using the proposed methodology are discussed.

INTRODUCTION

Large temperature contrasts phenomena and/or combustion, of materials used as flame retardants, UV protectors, antibacterial radiation, etc., result in the release of nano and micro particles. These particles are solid compounds of carbon that have not been completely burned and toxic compounds that are a threat to public health as they can cause respiratory problems.[2-5]

Typically, the fractal morphology of released aerosols in such processes is a physical property of interest for the study of formation of particles of different shapes, agglomerates, and identifying sources of these processes. As defined by Beniot Mandelbrot[6, 7], the main parameter is the fractal dimension (Df) and it can be successfully determined by various techniques such as image analysis using either scanning electron microscopy (SEM) or electron microscopy transmission (TEM), light scattering, or, concentration dependent studies, which are generally based on the mobility of the particles. When Df values are calculated in aggregates of combustion by numerical calculations or semi-empirical estimates, several factors, such as diameters of spheroids in aggregates, the distance and overlapping coefficients between two spheroids, the number of spheroids in an aggregate and the radius of gyration of an aggregate, should be considered[8, 9]. In general, these methods may introduce projection errors[10], although there are others which ignore this methodology[11-16].

The fBm analysis is obtained from the parameter known as fractal parameter of Hurst or simply Hurst coefficient[17].

$$B_H(t) = \frac{1}{\Gamma\left(\mathrm{H}+\frac{1}{2}\right)}\left\{\int_{-\infty}^{0}\left[\left(|t-s|^{H-\frac{1}{2}} - |s|^{H-\frac{1}{2}}\right)\right]dB(s) + \int_{0}^{t}\left[|t-s|^{H-\frac{1}{2}}\right]dB(s)\right\} \qquad (1)$$

where, $B_H(t)$ is a non-stationary Gaussian zero mean random function. In expression (1) Γ is the gamma function and when H = 1/2, fBm is reduced to brownian motion. Fluctuations in the textures of aggregates of soot due to combustion and the particles released by thermal shock can be represented by the $B_H(t)$ function, where t and s are two temporary variables. The value H is the Hurst coefficient and its value ranges from 0 to 1. Its relationship with the fractal dimension is $D_f = 2 - H$ for images in 2D. The fractal parameter H is evaluated by a fBm processor. This processor is fed by image processing programs[18, 19].

In this research, the fBm processor was used to obtain the value of fractal parameter H for the particles released by thermal shock and aggregate particles released by combustion.

Furthermore, the use of X-ray spectroscopy (EDS) and analysis of images obtained from SEM and TEM were combined to get an idea of how affect the release of elemental of chemicals into the environment.

EXPERIMENTAL METHODS AND MATERIALS

The methodology consisted of three steps: sampling of aerosols released by thermal shock or burned, analysis of elemental chemicals and morphology determination by the coefficient of Hurst to better understand the particle texture.

Ten samples of different materials were provided for research by the Technical Research Centre of Tampere, Finland (VTT), SO.F.TER Group of Forli, Italy and SAPSA Group of PEÑOLES, Mexico. All samples were prepared with functionalized nanoparticles from materials obtained by mining process with specific objectives. The materials that make up the samples are normally used as raw materials for construction, furniture, clothes, shoes, toys, etc. Table 1 shows the main characteristics of the samples, overall composition and their specific uses, which included: flame retardant, UV protector and bactericidal.

Table 1 Composition of samples used in the thermal shock and combustion experiments.

Sample Name	Type of Experiment	Matrix	Active Component	Use	Process Cycles
Target (100)	Thermal Shock	Chamber is empty, only with the steel supports	_	Experimental Reference	100
$Mg(OH)_2$+PP(5)	Thermal Shock	Polypropylene	$Mg(OH)_2$ (1%)	Flame Retardant	5
$Mg(OH)_2$+PP(50)	Thermal Shock	Polypropylene	$Mg(OH)_2$ (1%)	Flame Retardant	50
ZnO+PVC+Sawdust(5)	Thermal Shock	Polyvinyl Chloride and Sawdust	ZnO (1%)	UV Protection	5
Ag+PVC+Sawdust(5)	Thermal Shock	Polyvinyl Chloride and Sawdust	Ag (1%)	Bactericide	5
Ag(33%)+PP(20)	Thermal Shock	Polypropylene	Ag(33%)	Bactericide	20
Ag(15%)+PP(20)	Thermal Shock	Polypropylene	Ag(15%)	Bactericide	20
M1_831(Target)	Combustion	Polyvinyl Chloride (60%) Thermowood(40%)	_	_	1
M1_871	Combustion	Polyvinyl Chloride (60%) Thermo-wood (20%)	MHD micro(20%)	Bactericide UV Protect.	1
M1_872	Combustion	Polyvinyl Chloride (60%) Thermo-wood (20%)	MHD micro(10%) nano(10%)	Bactericide UV Protect.	1

Thermal shock testing was performed using a MIL-STD 2105D camera. This camera was used to control the temperature range and the number of cycles to be applied to samples. The temperature range used was between - 40 and 90°C. Cycles at 5, 20, 50 and 100 were used according to the time available to carry out the experiment and the number of samples. The time allotted for each cycle was 30 minutes. The cone calorimeter Fire Testing Technology of South West Research Institute (SwRI) at San Antonio, TX was used in combustion tests. The capture of particles and aggregates was performed using a MOUDI cascade type impactor (MOUDI ™ Model 100R, MSP Co., US). This equipment works at a flow rate of 30 ± 0.5 l/min. It has eight impaction stages with stage rotation. The analysis of the concentration of particles and aggregates was performed taking into account each of the cut-size diameters of the MOUDI impactor. Aerodynamic cut-size diameters have the following distribution (d50) 18, 10 (1), 5.6 (2) 3.2 (3) 1.8 (4) 1.0 (5) 0.56 (6) 0.32 (7) and 0.18 (8).

Figure 1 shows a simplified diagram of particles and aggregates capture during the thermal shock tests and combustion tests. Both, the particles and the aggregates were collected by a steel probe and then passed through a dilutor (model 100S VKL, Palas GmbH, Germany) in a modified chamber to dilute to a ratio of 1:2000 with air pre-treated with high efficiency filters (HEPA) and a column of activated carbon. The dilution air had a temperature of 25^{o}C and a relative humidity of 50%. To reduce moisture interference, mica filters were conditioned at a relative humidity of 40% and 20 to 25°C for 24 h before the SEM/EDS (or X-Ray microanalyses) observation. Although the lowest cut-size diameter for the MOUDI 100R impactor was 0.18 µm, particles with aerodynamic diameters less than 2 nm were detected.

Figure 1. Aggregates and particles sampling scheme.

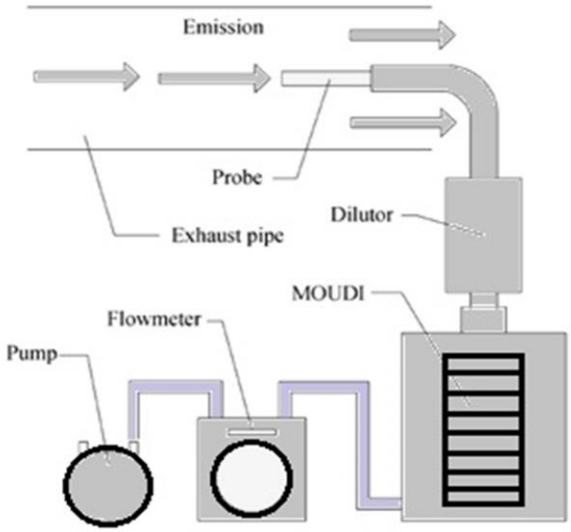

In the case of aggregates sampling produced from combustion, soot deposition on the mica filters was very abundant. Therefore, careful removal of the particles was performed using ultrasound to obtain definition, without loss of original fractals parameters on digital images in 2D. The observations were performed using a field emission SEM with a narrow beam of 1 nm (JEOL JSM 7401F).

Subsequently, the digital brightness level grayscale images from the SEM (magnification x 10^5) were automatically parameterized as a function of mathematical matrix. The window size for the texture analysis depended on aggregate size in the case of complete burning of samples. Figure 2(a) presents the size of the segmentation of a global image that can be increased from 65 × 65 to 80 × 80 pixels with equimultiple as a software setting.

Furthermore, taking into account the exclusion of the uniform background produced for the mica filter, sampling was conducted taking 2 or 4 regions which partially covered the overlap

Fig 2 SEM images and H mapping for (a) particles and (b) aggregates.

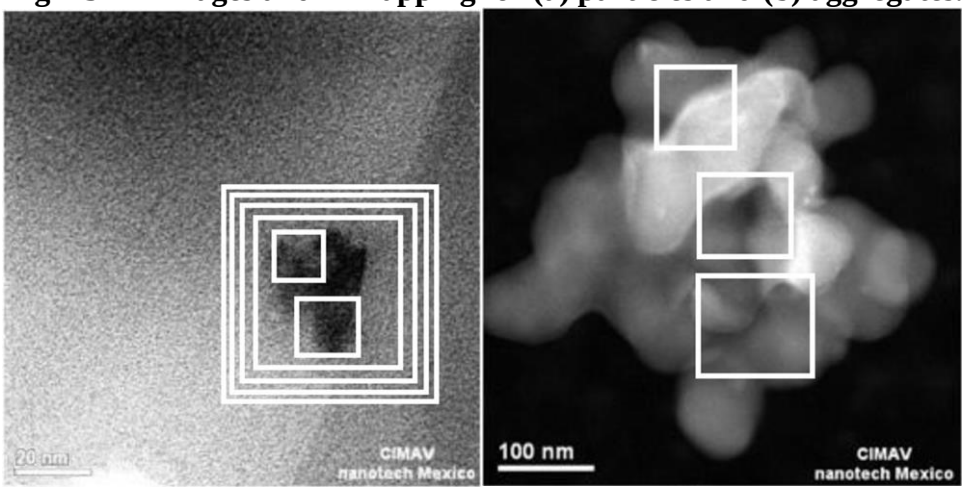

(a) **(b)**

region of the spheroids in each image. In this way, was easy to calculate the average value of H with the fBm processor. The same procedure was used for particles and aggregates, as observed in Figures 2(a) and 2(b) respectively. The elements with low atomic number (6-92) embedded in both particles and aggregates were determined qualitatively and quantitatively by their spectra SEM/EDS. Each microscope has an EDS probe. A small acceleration voltage of 10 kV was chosen to eliminate interference caused by the background and deformation caused by overheating of the structure of the particles and aggregates to avoid collapsing or lumpy states. A collection time of 128 s to enhance the accumulation of the signal at each sample was used. Because the focus diameter and depth of X-ray beam was about 0.5 µm, background interference must be eliminated for ESD detection in aggregates with a diameter > 1 µm.

RESULTS AND DISCUSSION

All experimental results were close to average diameters of spherules and particles reported in the range of 20-35 nm under different operating conditions by Neer and Koylu[20]. Figure 3(a) and 3(b) show the results of standard modes mass distribution obtained in the eight stages of the MOUDI impactor in both experiments. As illustrated in Figure 3(a), two main modes are obtained in the log-normal distribution (dC/CtlogDp) vs. logarithm of aerodynamic diameter of the particle for thermal shock tests. The first mode is located in the region below 0.18 µm (180 nm) and the second mode is between 0.32 and 0.56 µm. Each one has a value of 32% and 31% per particle diameter in nanometers, respectively. For combustion testing by calorimetry, two main modes of log-normal distribution, one in the region below 0.18 µm and the other between 0.56 and 1.0 µm were also obtained. Figure 3(b) shows clearly each with values of 40.3% and 18% per particle diameter in nanometers, respectively. In both experiments, the predominant particles were PM1 (below 1000 nm) according to Figure 3.

Figure 3. Mass distribution modes of particles and aggregates for (a) Thermal Shock tests and (b) Combustion by cone calorimeter tests.

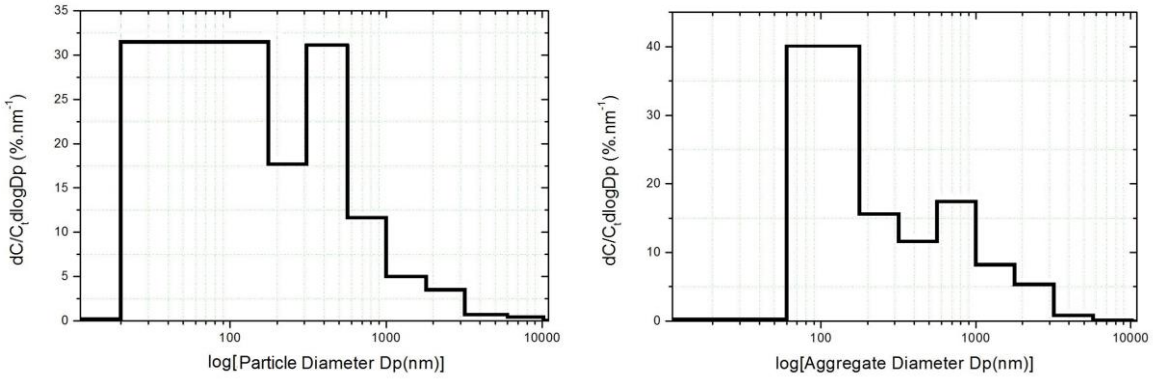

(a) **(b)**

Table 2 shows the average values of H in each one of the samples that released particles and aggregates as analyzed by SEM. The number of particles and aggregates analyzed (N_{PA}), released in each sample was in the range of 12 to 44. The number of segmentation windows (NW) for each sample was in the range of 39 to 176. The values depend on the size of the particle or aggregate. H uncertainties were high in all samples. The variation coefficients (V_C)

ranged between 18% and 67%. The highest value occurred in the sample Target of the thermal shock experiment, despite the hermeticity of the camera. None of the particles belonged to any sample. Each detected particle may have come from the chamber walls or holders.

Because fractal dimension Df = 2 - H, small values of H result in large D_f. A small H value near zero indicates that the segmented texture of the image fluctuates markedly [21]. Fluctuation implies the appearance of increased roughness in the overlapping region of primary spheroids. Therefore, the texture roughness increases as H decreases. This result can be confirmed by the DLCA calculation[22]. Because the morphology of aggregates can influence their reactive and toxicological properties, our results implied that the Hurst coefficient should be considered in future particles release studies.

Table 2. Analyzed samples parameters: mean values of fractal parameter H, standard deviation (SD) and variation coefficient [VC = (σ_s/H)×100]

Emission Source	N_{PA}	N_W	H	SD	VC
Target (100)	12	47	0.6	0.4	67
$Mg(OH)_2$+PP(5)	32	125	0.5	0.2	40
$Mg(OH)_2$+PP(50)	42	125	0.4	0.2	50
ZnO+PVC+Sawdust(5)	22	67	0.4	0.3	75
Ag+PVC+Sawdust(5)	13	39	0.3	0.1	33
Ag(33%)+PP(20)	16	48	0.28	0.05	18
Ag(15%)+PP(20)	14	42	0.27	0.07	26
M1_831(Target)	42	116	0.30	0.07	23
M1_871	44	176	0.5	0.2	40
M1_872	23	65	0.4	0.1	25

Figure 4 shows the distribution of values of H in the different samples used in (a) thermal shock and (b) combustion. It seems that the sudden temperature changes result in higher release of nanoparticles, as shown in Figure 4(a). Furthermore, the use of nanoparticles tends to decrease the value of H. The decrease in H results in higher statistical noise. The series of contrasts of gray tend to lose uniformity, become more chaotic, and cease to be persistent. Increasing nanoparticle content within the particles of the samples causes the released particles to have rougher surfaces with increasingly sharp edges.

The opposite occurs in the total combustion experiments with the appearance of soot. While use of nanoparticles is greater, the combustion processes tend to reduce the roughness of the aggregates. The carbon emissions increase in relation to other elements. These results are in agreement with the work presented by Herrera et al. in the IT3-2014 conference[23] where they showed that nanoparticles tend to remain in the ashes of the combustion products and generally are not released into the environment.

The results of the elemental analyses are shown by EDS microscopic systems. Table 3 shows the average content of the various chemical elements that make up each sample. These values are reported in % dry weight (w/w) for each of the EDS analyses on each particle and aggregate. The column value Dp (μm) represents the average aerodynamic diameter of particles processed by EDS.

Figure 4. Mean H values for the different types of samples analyzed in (a) particles and (b) aggregates. Error bars represent the relative standard deviation.

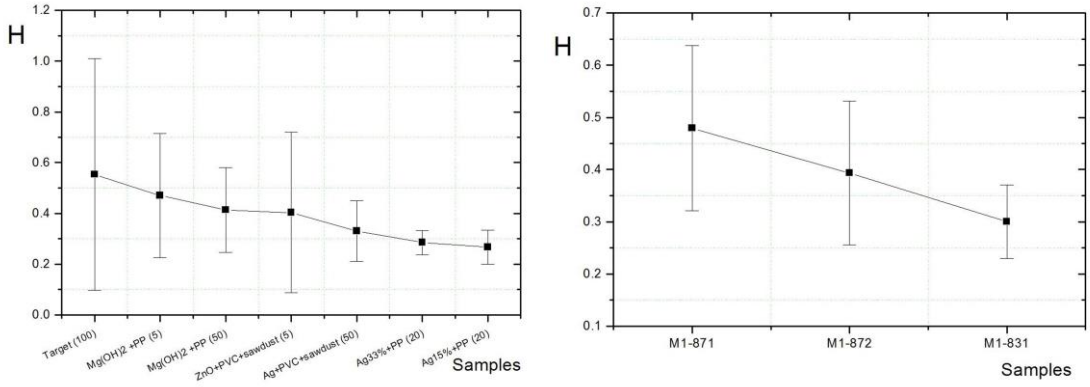

(a) **(b)**

Table 3. Chemical composition results in % dry weight (w/w) for each of the samples analyzed by EDS.

Sample Name	Exp	Dp(μm)	C	O	Mg	Al	Si	P	S	Cl	K	Ti	Cr	Fe	Ni	Cu	Zn	Pb
Target (100)	TS	**0.6**	**87**	**13**	**0.6**	_	**0.2**	**5.4**	_		_	**26**	**1.6**	_	_	_	_	_
$Mg(OH)_2$+PP(5)	TS	**0.4**	**70**	**23**	**0.7**	**0.5**	**1.9**	**0.4**	**0.8**	**0.4**	**0.5**	_	**0.6**	**0.7**	**0.3**	_	**0.5**	_
$Mg(OH)_2$+PP(50)	TS	**0.3**	**63**	**21**	**13**	**1.1**	**4.3**	**0.2**	**2.4**	**0.5**	**0.4**	**5**	_	_	_	_	**7**	_
ZnO+PVC+Sawdust(5)	TS	**0.8**	**51**	**23**	_	_	**2.2**	_	**4.9**	**1.9**	**1.4**	**3.5**	**1.2**	**0.6**	_	_	**28**	**4**
Ag+PVC+Sawdust(5)	TS	**0.4**	**86**	**17**	_	**10**	**1.1**	_	_		_	_	**15**	**58**	**6**	_	_	_
Ag(33%)+PP(20)	TS	**0.5**	**85**	**12**	**0.9**	_	**0.4**	**4.5**	_		**0.4**	_	**0.7**	_	_	_	_	_
Ag(15%)+PP(20)	TS	**1.0**	**88**	**16**	**0.4**	_	**4.4**	**2.5**	**0.3**		**0.4**	_	**0.4**	**0.6**	_	_	_	_
M1_831	COM	**0.6**	**81**	**6**	_	_	**2.5**	**0.2**	_	**0.7**	**0.2**	_	_	_	_	_	**0.1**	_
M1_871	COM	**0.7**	**85**	**8**	_	**0.5**	_	_	_	**8.5**	_	_	_	_	_	**20**	**2.6**	_
M1_872	COM	**0.3**	**91**	**2**	_	_	**8.7**	_	_	**1.1**	**0.6**	_	**0.1**	_	_	**31**	**0.6**	_

–: Non-detectable

It is noteworthy that each of the average diameters shown in Table 3 fall within the main statistical modes of Figures 3(b). Table 3 also shows that there is release of functionalized Zn and Mg nanoparticles in the samples investigated in the MINANO project. Chemical elements cited appear in Mg samples of $Mg(OH)_2$+PP(50) and ZnO+PVC+Sawdust (5) with 13%$_{wt}$ of Mg and 28%$_{wt}$ of Zn. Random appearances of Cu in M1_871 Cu (20%$_{wt}$) and M1_872 (31%$_{wt}$) could be due to the structure of the grids of the samples for SEM/TEM. Other elements appear but only in tenths of a percent concentration, except for Ti on Target sample due to the walls of the chamber. Figure 5(a) and 5(b) show the peaks of Mg and Zn in XRF spectra obtained by EDS.

Figure 5. XRF Spectra for samples $Mg(OH)_2$ + PP (50) and ZnO + PVC + Sawdust (5)

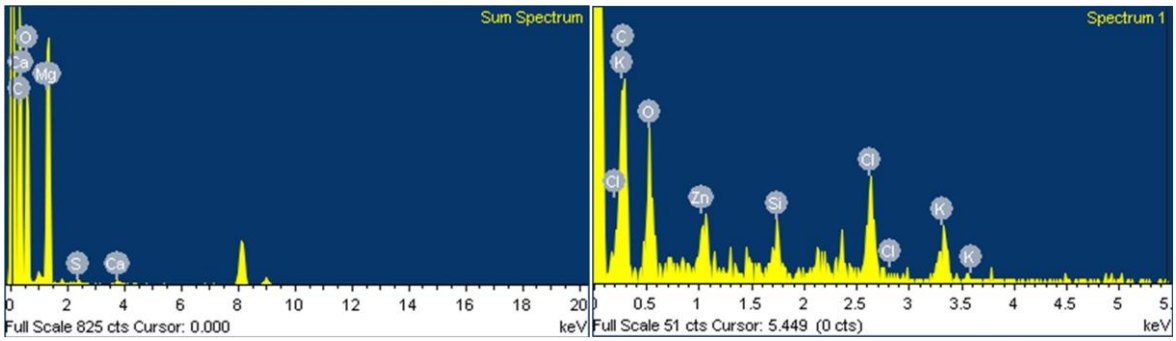

(a) (b)

SUMMARY

The use of fBm extraction and SEM/EDS detection were combined to investigate the fractal morphology and elemental chemical composition of ten samples of nanocomposites functionalized for industrial and environmental purposes. Several of the contributions derived from our results are summarized as follows:

(1) The particulate matter rate (PM_1/PM_{10}) was 10 times in the thermal shock experiments and 5 in the combustion. This result corroborates the adverse impact that particle release can have on health due to the small diameters of the released particles.

(2) Fractal information for particles and aggregates can be determined by the H parameter that varies from 0 to 1 and is related to Df through a simple mathematical equation, Df = 2 – H, for SEM images 2D. H values for particulate thermal shock experiments were between 0.6 and 0.27 and aggregates in combustion experiments between 0.3 and 0.5. This experimental result is in agreement with others reported only using TEM.

(3) The average value of H in thermal shock, obtained by means 2D SEM image, grows when nanoparticles functionalized particles are used. This results in increased roughness in the texture of the particles. The opposite occurs in aggregates released in combustion processes.

(4) Nanoparticles are released, with relatively high concentration of Zn and Mg in the samples $Mg(OH)_2$+PP(50) and ZnO+PVC+Sawdust(5) used in the experiments of thermal shock. There was no release of nanoparticles in the samples used in the experiments of combustion because the elements which appear functionalized nanoparticles remain in the ash.

ACKNOWLEDGEMENTS

We gratefully acknowledge support by project MINANO, research cooperation among different institutes of the European Union and Latin America institutes (SAPSA, especially to Ph. D Ricardo Benavides), (OWENS), (CIQA), (UASLP) and (CIMAV).

A special acknowledgment to Professor Mika Paajanen VTT from Finland, chairman, for allowing us to participate in such an instructive exercise and also to Professor Stig Olsen DTU from Denmark for recommending the calculations of the life cycles analysis of the nanoparticles used in the entire project.

REFERENCES

1. MINANO, Project Number: 263946, Call part identifier: FP7-NMP-2010-EU-Mexico
2. Basfar, A. *Effect of various combinations of flame-retardant fillers on flammability of radiation cross-linked poly(vinyl chloride) (PVC).* 2002, Polymer Degradation and Stabilit , 333-340.
3. Laoutid, B. A. *New prospects in flame retardant polymer materials: From fundamentals to nanocomposites.* 2008, Material Science and Engineering, 100-125.
4. Zhang, J.; Delichatsios, M.; & Bourbigot, S. *Experimental and numerical study of the effects of nanoparticles on pyrolysis of a polyamide 6 (PA6) nanocomposite in the cone calorimeter*. 2009, Combustion and flame, 2056-2062
5. Zhang, Z.; Zhang, J., Lu, B.-X.; Xiang, Z., Kang, C., & Kim, J. *Effect of flame retardants on mechanical properties, flammability and foamability of PP/wood–fiber composites*. 2011, COMPOSITES, 150-158.
6. Mandelbrot, B.B., Van Ness, J.W., 1968. Fractional Brownian motion, fractional noises and application. SIAM Reviews 10, 422–437.
7. Mandelbrot B B, 1983. Fractals: Form, Chance and Dimension. San Francisco, USA: W. H. Freeman and Co.
8. Wentzel, M.; Gorzawski, H.; Naumann, K. H.; Saathoff, H. and Weinbruch, S. *Transmission electron microscopical and aerosol dynamical characterization of soot particles*. 2003, Journal of Aerosol Science, 34: 1347–1370.
9. Park K, Kittelson D B, Mc Murry P H, 2004. Structural properties of diesel exhaust particles measured by transmission electron microscopy (TEM): relationships to particle mass and mobility. *Aerosol Science and Technology*, 38: 881–889
10. Rogak, S. N.; Flagan; R C. *Characterization of the structure of agglomerate particles*. Particle and Particle System Characterization, 1992, 9: 19–27.
11. Gwaze P, Schmid O, Annegarn H J, Andreae M O, Huth J, Helas G,. *Comparison of three methods of fractal analysis applied to soot aggregates from wood combustion*. Journal of Aerosol Science, 2006,37: 820–838.
12. Jennane, R.; Harbaa, R.; Lemineura; G.; Bretteila, S.; Stradeb, A. and Laurent, C. Estimation of the 3D self-similarity parameter of trabecular bone from its 2D projection. 2012, Archives-Ouvertes, HAL.
13. Luo C. H.; Wen C. Y.; Liaw J. J.; Chiu S. H.; Lee W. M. Texture characterization of atmospheric fine particles by fractional Brownian motion analysis. 2004, *Atmospheric Environment*, 38: 935–940.

14. Luo, C. H.; Lee, W. M.; Lai; Y. C.; Wen, C. Y.; Liaw J. J. Measuring the fractal dimension of diesel soot agglomerates by fractional Brownian motion processor. 2005a, Atmospheric Environment, 39: 3565–3572
15. Luo C. H., Chuang L. C., Wen C. Y., Liaw J. J.,. *Projected texture characteristics of allergenic bioaerosols (pollens)*. 2005b, Journal of the Chinese Institute of Environmental Engineering, 15: 199–204.
16. Luo, C. H.; Lee, W. M.; Liaw, J. J. Morphological and semi-quantitative characteristics of diesel soot agglomerates emitted from commercial vehicles and a dynamometer. 2008 DOI: 10.1016/S1001-0742(08)62291-3
17. Wen C Y, Acharya R, 1998. Self-similar texture characterization using a Fourier-domain maximum likelihood estimation method. *Pattern Recognition Letters*, 19: 735–739.
18. Sage, D. and Unser M.;, *"Teaching Image-Processing Programming in Java"*, IEEE Signal Processing Magazine, vol. 20, no. 6, pp. 43-52, November 2003
19. Karperien, Home Page Box Counting http://rsb.info.nih.gov/ij/plugins/fraclac/FLHelp-/BoxCounting.htm#sampling. (accessed December 2012).
20. Neer, A. and, Koylu, U. O. Effect of operating conditions on the size, morphology, and concentration of submicrometer particulates emitted from a diesel engine. *Combustion and Flame*, 2006, 146: 142–154.
21. Fortin C, Kumaresan R, OhleyW, Hoefer S, 1992. Fractal dimension in the analysis of medical images. *IEEE Engineering in Medicine and Biology*, June: 65–71.
22. Oh, C. and Sorensen, C. M. *The effect of overlap between monomers on the determination of fractal cluster morphology*. Journal of Colloid and Interface Science, 193: 1997, 17–25.
23. Herrera, E. F.; Navarro C. J.; Espinoza, M. A.; Carrasco, L.; Gonzalez, G.; Roman M., Montelongo, M.; Ramírez, E., Carrillo, J. I.; Campos, A. and Gómez, R. *Physicochemical Study of the Products of Combustion and Thermal Shock on Polymeric Materials*. 33rd International Conference on Thermal Treatment Technologies & Hazardous Waste Combustor. Paper # (9). October 13-15, 2014

KEYWORDS

MINANO Project, nanoparticles, fractal parameters, Coefficient of Hurst, nanocompounds, particles, aggregates, flame retardant, UV protection, bactericidal.